

1 **Precipitation stable isotopic signatures of tropical cyclones in Metropolitan**
2 **Manila, Philippines show significant negative isotopic excursions**

3
4 Dominik Jackisch¹, Bi Xuan Yeo², Adam D. Switzer^{1,2}, Shaoneng He¹, Danica Linda M.
5 Cantarero³, Fernando P. Siringan³ and Nathalie F. Goodkin^{1,2,4}
6

7 ¹ Earth Observatory of Singapore, Nanyang Technological University, Singapore
8 639798

9 ² Asian School of the Environment, Nanyang Technological University, Singapore
10 639798

11 ³ Marine Science Institute, University of the Philippines Diliman, Quezon City 1101,
12 Philippines

13 ⁴ American Museum of Natural History, New York 10024, USA
14

15 Correspondence to: Adam D. Switzer (aswitzer@ntu.edu.sg)
16

17 **Abstract**
18

19 Tropical cyclones have devastating impacts on the environment, economies, and societies,
20 and may intensify in the coming decades due to climate change. Stable water isotopes serve
21 as tracers of the hydrological cycle, as isotope fractionation processes leave distinct
22 precipitation isotopic signatures. Here we present a record of daily precipitation isotope
23 measurements from March 2014 to October 2015 for Metropolitan Manila, a first of a kind
24 dataset for the Philippines and Southeast Asia. We show that precipitation isotopic variation
25 at our study site is closely related to tropical cyclones. The most negative shift in $\delta^{18}\text{O}$ value
26 (-13.84 ‰) leading to a clear isotopic signal was caused by Typhoon Rammasun, which
27 directly hit Metropolitan Manila. The average $\delta^{18}\text{O}$ value of precipitation associated with
28 tropical cyclones is -10.24 ‰, whereas the mean isotopic value for rainfall associated with
29 non-cyclone events is -5.29 ‰. Further, the closer the storm track to the sampling site, the
30 more negative the isotopic values, indicating that in-situ isotope measurements can provide
31 a direct linkage between isotopes and typhoon activities in the Philippines.

32 1. Introduction

33

34 The Philippine archipelago, with its fast-growing population clustered along the coastline, is
35 one of the most vulnerable countries to climate change (Cinco et al., 2014). It is especially
36 prone to the devastating effects of tropical cyclones. Thus, it is considered a hotspot region
37 for hydrometeorological disasters (Cinco et al., 2014; Cruz et al., 2013; Takagi and Esteban,
38 2016). There is a clear need for developing a better understanding of tropical cyclone (TC)
39 dynamics and cyclone histories in the context of prediction that may allow government
40 agencies to implement proper mitigation and adaptation policies. Nine TCs per year made
41 landfall on average between 1951 to 2013 in the Philippines. The number of TCs not making
42 landfall but reaching Philippine waters is substantially higher with 19.4 per year (Cinco et al.,
43 2016). Changing climate and associated warming of the surface ocean, will likely increase the
44 intensity of tropical cyclones in the future (Emanuel, 2005; Webster and Holland, 2005;
45 Woodruff et al., 2013).

46

47 The Philippines was struck by several devastating TCs in recent years (Table 1). Typhoon
48 Haiyan (2013), which tracked over the Visayas has been the costliest TC to date (~ 2.06 billion
49 USD in 2013), with strong winds and intense storm surges inundating coastal areas resulting,
50 in more than 6000 fatalities (Alojado and Padua, 2015; Lagmay et al., 2015; Soria et al., 2016).
51 Typhoon Rammasun, which made landfall in July 2014, is ranked number 3 with ~ 880 million
52 USD in 2014 (Alojado and Padua, 2015; NDRRMC, 2014). Eighty percent of the strongest
53 typhoons making landfall in the Philippines over the last three decades developed during
54 higher than average sea surface temperatures (SST), which supports the hypothesis that TC
55 intensities are projected to rise in the future with an increase in global temperatures (Guan
56 et al., 2018; Webster and Holland, 2005; Takagi and Esteban, 2016). For example, SST was
57 found to be anomalously high and reaching 29.6 °C during the formation of Typhoon Haiyan
58 (Takagi and Esteban, 2016). The average Philippines' ocean SST for the period from 1945 to
59 2014 (basin between 6° – 18° N, 120° – 140° E) is ~ 28.5 °C based on National Oceanic and
60 Atmospheric Administration Extended Reconstructed Sea Surface Temperature Dataset,
61 Version 5 (NOAA ERSST v5) (Takagi and Esteban, 2016). By the end of the 21st century, average
62 typhoon intensity in the low-latitude northwestern Pacific is predicted to increase by 14 %
63 due to rising ocean temperatures (Mei et al., 2015).

64

65 A few studies have demonstrated the potential to investigate tropical cyclones using stable
66 water isotopes (Good et al., 2014; Lawrence et al., 2002; Munksgaard et al., 2015; Pape et al.,
67 2010). As dynamic tracers of hydrological processes, stable water isotopes ($\delta^2\text{H}$ and $\delta^{18}\text{O}$) can
68 provide insights into the water and energy budgets of TCs (Good et al., 2014; Lawrence and
69 Gedzelman, 1996). In the regions with general TC occurrence, significantly lower $\delta^2\text{H}$ and $\delta^{18}\text{O}$
70 are associated with TC rainfall due to strong isotope fractionation processes, compared to
71 other tropical rain events (Lawrence, 1998; Lawrence and Gedzelman, 1996). Furthermore,
72 $\delta^2\text{H}$ and $\delta^{18}\text{O}$ have been used successfully to interpret TC history from paleoarchives, such as
73 tree rings and speleothems (Oliva et al., 2017). For instance, tree-ring cellulose isotope
74 proxies have recorded the recent 220 years of cyclones in the southeastern USA (Miller et al.,
75 2006); similarly, high-resolution isotopic analysis of tree-rings from the eastern US revealed
76 the occurrence of hurricanes in 2004 (Li et al., 2011); a 23-year stalagmite record from Central
77 America was used to reconstruct past TC activity (Frappier et al., 2007), and isotope signals
78 from a 800-year stalagmite record were used to reconstruct past TC frequencies in
79 northeastern Australia (Nott et al., 2007). Interpretation of TC history in paleotempestology
80 from paleoarchives is based on the fact that TCs leave distinct isotopic signatures on
81 precipitation, possibly providing information on TC's evolution and structure (Lawrence et al.,
82 2002).

83

84 The depletion in stable isotopes has been attributed to the high condensation levels, strong
85 isotopic exchanges between inflowing water vapour and falling raindrops in cyclonic rainfall
86 bands, resulting in a temporal decrease of isotopic values throughout a rain event (i.e.
87 amount effect) (Lawrence, 1998; Lawrence and Gedzelman, 1996). Isotopic depletion can be
88 further enhanced by TC's thick, deep clouds, relatively large storm size and longevity
89 (Lawrence, 1998). Furthermore, while isotopic depletion increases inwards towards the eye
90 wall of the storm (Lawrence and Gedzelman, 1996), isotope ratios inside the inner eye wall
91 region are relatively enriched, likely due to an intensive isotopic moisture recharge with heavy
92 isotopes from sea spray (Fudeyasu et al., 2008; Gedzelman et al., 2003). These findings are
93 based on work conducted in the 1990s in Puerto Rico and on the southern and eastern coasts
94 of the United States. More recently, these previous findings have been confirmed by studying
95 TCs which occurred in a few other regions, such as in China or Australia (Chakraborty et al.,

96 2016; Fudeyasu et al., 2008; Good et al., 2014; Munksgaard et al., 2015; Xu et al., 2019).

97

98 The above-mentioned studies are geographically limited to a few locations globally, with no
99 studies in Southeast Asia and the Philippines in particular. Here, we present the first such
100 study for the Philippines, with daily isotope measurements of precipitation from
101 Metropolitan Manila (the National Capital Region) spanning from March 2014 to October
102 2015. During the study period, nine tropical cyclones passed by or made landfall within 500
103 km of the sampling site (Fig. 1). The main objectives of this research are the following:

- 104 - To understand if there is an isotopic variation in precipitation associated to the TC
105 landfall in the Philippines and if tropical cyclones leave clear isotopic signals.
- 106 - To identify the isotopic signals measured for Metropolitan Manila and the intensity of
107 the isotopic depletion associated to TC activities, and to identify how it is represented
108 spatially.
- 109 - To understand the isotopic variation with distance from the TC track in the Philippines.

110 Our findings provide a baseline dataset for reconstruction of typhoon activities using stable
111 isotopes and contribute to a better understanding of past and future TC activities in the
112 Philippines.

113

114

115 **2. Materials and methods**

116

117 **2.1 Site description**

118

119 The Philippines is a Southeast Asian country comprising more than 7000 islands located in the
120 Northwest Pacific between 4° 40' N and 21° 10' N, and 116° 40' E and 126° 34' E (Fig. 1). The
121 country experiences an average annual rainfall of about 2000 mm, influenced by two
122 monsoon seasons, the northeast monsoon from November to April and the southwest
123 monsoon from May to October (Cinco et al., 2014). About 35 % of the annual rainfall is related
124 to TC activity, while its contribution rises to about 50 % for Luzon and decreases to 4 % for
125 the southern island of Mindanao (Cinco et al., 2016). Part of the rainfall amount in the
126 Philippines is of orographic nature due to north-south oriented mountain ranges of more than
127 1000 m spanning the largest islands of Luzon and Mindanao (Villafuerte et al., 2014). The

128 majority of the steadily growing population in the Philippines (101 million 2017 census) live
129 in densely populated, low-elevation areas close to the coastlines (Cinco et al., 2014, 2016;
130 Philippine Statistics Authority, 2017).

131

132

133 **2.2 Isotopic data**

134

135 In total, 186 daily precipitation samples were collected from 11 March 2014 to 27 October
136 2015 using a PALMEX collector (Gröning et al., 2012) at the Marine Science Institute of the
137 University of the Philippines Diliman located in Quezon City, which is a part of Metropolitan
138 Manila. The rain station was installed on the rooftop of the Marine Science Institute
139 (14°39'02.5"N, 121°04'08.6"E), which is centrally situated in the campus and surrounded by
140 trees and various green spaces. The rooftop location proved ideal for rainwater collection as
141 it allowed for unobstructed access to rainwater without any potential sources of
142 contamination. Samples were collected daily at 10 am and transferred without headspace to
143 30-ml HDPE bottles for storage prior to analysis. Samples were sent to the Earth Observatory
144 of Singapore, Nanyang Technological University, Singapore and were analysed for stable
145 isotopes using a Picarro L1230-*i* laser spectroscopy instrument. We followed the procedures
146 described by Van Geldern and Barth (2012) for post-run corrections and calibration. Three in-
147 house water standards used for calibration include KONA (0.02 ‰ of $\delta^{18}\text{O}$; 0.25 ‰ of $\delta^2\text{H}$),
148 TIBET (-19.11 ‰ of $\delta^{18}\text{O}$; -143.60 ‰ of $\delta^2\text{H}$), and ELGA (-4.25 ‰ of $\delta^{18}\text{O}$; -27.16 ‰ of $\delta^2\text{H}$).
149 They are calibrated against the international reference water VSMOW2 and SLAP2. Long-term
150 analysis of our QA/QC standards yields precision of 0.04 ‰ for $\delta^{18}\text{O}$ and 0.2 ‰ for $\delta^2\text{H}$. We
151 used $\delta^{18}\text{O}$ and $\delta^2\text{H}$ to calculate deuterium excess, which is defined as $d\text{-excess} = \delta^2\text{H} - 8 * \delta^{18}\text{O}$
152 and is commonly regarded to reflect evaporation conditions of moisture source regions.

153

154 **2.3 Cyclone track data**

155

156 The International Best Track Archive for Climate Stewardship (IBTrACS) dataset contains
157 global TC best-track data and is a joint effort of various regional meteorological institutions
158 and centres that are part of the World Meteorological Organization (WMO). The data is
159 publicly available, and comprises information on storm eye/centre with its coordinates, wind

160 speed, and pressure, etc., with a temporal resolution of six hours (Knapp et al., 2010; Rios
161 Gaona et al., 2018). Apart from visualization of cyclone paths, we used the dataset to calculate
162 the spatial distance between the storm's eye coordinates and our sampling site.

163

164 **2.4 Satellite precipitation data**

165

166 We used the IMERG Version 5 Final daily product, a remotely-sensed precipitation dataset
167 from satellites to highlight cyclonic tracks and precipitation patterns of several TC's passing
168 by Metropolitan Manila, and to identify which rainfall events were not affected by cyclonic
169 activity, and instead were associated with local or other regional convection activities. Such
170 dataset is beneficial as it provides quasi-global grid-based rainfall estimates for land and the
171 oceans (Poméon et al., 2017). The Integrated Multi Satellite Retrievals for GPM (IMERG) from
172 the Global Precipitation Measurement (GPM) programme with a fine 0.1-degree grid size
173 (Huffman et al., 2017) has been available since March 2014, and provides precipitation data
174 in different temporal resolutions, such as half-hourly or daily. Such satellite rainfall data has
175 been previously utilized to show TC tracks and related rainfall intensities (Rios Gaona et al.,
176 2018; Villarini et al., 2011).

177

178 **2.5 Rainfall, temperature and relative humidity data**

179

180 Daily rainfall, mean daily relative humidity and mean daily temperature data was obtained
181 from the Philippine Atmospheric, Geophysical and Astronomical Services Administration
182 (PAGASA), which maintains a rainfall monitoring station about 2.7 km away from our sampling
183 site. The data is freely available for the period 2013 to 2017 and can be accessed on the
184 Philippines Freedom of Information website (www.foi.gov.ph).

185

186

187 **3. Results**

188 **3.1 Isotopic variation of stable isotopes in daily precipitation**

189

190 One hundred and eighty-six daily precipitation samples were collected during the 19 months
191 of the study period spanning from 11 March 2014 to 27 October 2015 in Metropolitan Manila.

192 Their stable isotope compositions show large seasonal isotopic variability; $\delta^{18}\text{O}$ ranges from
193 4 ‰ to -13.84 ‰, and $\delta^2\text{H}$ from 16.84 ‰ to -99.1 ‰ (Fig. 2). The highest $\delta^{18}\text{O}$ of 4 ‰ was
194 observed on 9 April 2014 during the annual dry period, whereas the lowest $\delta^{18}\text{O}$ of -13.84 ‰
195 was observed on 16 September 2014 in association with TC activity. The mean $\delta^{18}\text{O}$ of
196 precipitation at the study site is -5.29 ‰ for non-TC rain systems, while TCs, as large regional
197 convective systems, have the potential to cause a change in δ -values of up to almost 9 ‰
198 relative to the mean. The average $\delta^{18}\text{O}$ of the nine TCs that tracked within <500 km from the
199 sampling site is -10.24 ‰ (STDEV of 2.11), a factor of 2 larger than the mean from non-TC
200 precipitation (average is -5.29 ‰, STDEV of 2.64).

201

202 An inter-annual variation of stable isotopes in precipitation is observed in the time series of
203 Metropolitan Manila, where the generally humid summer months are characterized by heavy
204 rainfall and exhibit lower isotope values compared to the rest of the year (Fig. 2). The
205 precipitation isotopes are characterized by slightly higher values during winter and spring,
206 when temperatures and relative humidity are lower with less frequent rainfall. Especially
207 early 2015 shows drier conditions with sporadic rainfall and relative humidity levels of about
208 60 % to 70 %. This is also reflected in the precipitation collected on 1 March 2015 with $\delta^{18}\text{O}$
209 of 0.01 ‰ and $\delta^2\text{H}$ of 9.8 ‰, respectively. Although d-excess shows relatively high temporal
210 variability, ranging from -15.18 ‰ to 24.31 ‰, it largely clusters in a small range between 5
211 ‰ to 15 ‰.

212

213 Based on the daily isotope measurements of rainfall events between 2014 and 2015, we
214 determined the LMWL (local meteoric water line) for the study site as $\delta^2\text{H} = 7.2674 \times \delta^{18}\text{O} +$
215 5.4103 (Fig. 3), indicating that slope and intercept of the LMWL are lower due to the influence
216 of tropical precipitation compared to the GMWL (global meteoric water line) with $\delta^2\text{H} = 8 \times$
217 $\delta^{18}\text{O} + 10$ (Craig, 1961).

218

219 In order to assess meteorological controls on the isotopic composition of daily precipitation
220 at Metropolitan Manila, we investigated the correlation between $\delta^{18}\text{O}$, daily precipitation
221 amount, daily mean temperature, and daily mean relative humidity. Additionally, $\delta^{18}\text{O}$ is
222 compared to d-excess (n=187) (Fig. 4). We found that $\delta^{18}\text{O}$ is weakly correlated to d-excess

223 ($R^2=0.2187$), precipitation amount ($R^2=0.1087$), and relative humidity ($R^2=0.1323$). No
224 association is observed between $\delta^{18}\text{O}$ and temperature ($R^2=0.0338$).

225

226 In order to get further insights into the seasonal variations, we also calculated the average
227 values for each month in the time series for every isotopic and climatic parameter, while
228 rainfall is reported as monthly totals (Table 2). $\delta^{18}\text{O}$ is relatively low during the summer
229 months, for instance with -7.29‰ in September 2014 compared to the months of winter and
230 spring with -0.53‰ in April 2014 or -0.66‰ in February 2015. Similarly, the monthly rainfall
231 total is less in winter and spring with 19.2 mm in March 2014 and 29.2 mm in January 2015
232 compared to the summer months such as July and August 2014 with 455.4 mm and 420.7 mm
233 respectively. As mentioned before regarding the daily measurements, we also observe on the
234 monthly scale conditions which are more humid in the summer. We investigated the
235 relationship between the isotopic composition of precipitation ($\delta^{18}\text{O}$) and meteorological
236 parameters (total monthly rainfall, average relative humidity, and temperature) on a monthly
237 scale. $\delta^{18}\text{O}$ and $\delta^2\text{H}$ are strongly correlated (Pearson correlation coefficient) with $r=0.96$
238 ($n=18$, $p\text{-value}<0.0001$ and 99% confidence level), whereas the relationship between $\delta^{18}\text{O}$
239 and d-excess yields an r of -0.64 ($n=18$, $p\text{-value}=0.003$). A clear negative correlation was
240 determined between $\delta^{18}\text{O}$ and precipitation with $r=-0.67$ ($n=18$, $p\text{-value}=0.002$) and between
241 $\delta^{18}\text{O}$ and relative humidity with $r=-0.85$ ($n=18$, $p\text{-value}<0.0001$). $\delta^{18}\text{O}$ and temperature are
242 not correlated with $r=0.04$ ($n=18$, $p\text{-value}=0.87$).

243

244 A relationship between isotopic value and the distance of the TC towards the sampling site
245 was found. The TCs' distance of up to 500 km to sampling site and the precipitation isotope
246 value are correlated with $r=0.55$ ($n=16$, $p\text{-value}<0.05$ and 99% confidence level). This
247 relationship weakens with an increase in the distance from the sampling site: a distance of
248 500 to 1000 km yields an r of 0.2 ($n=19$, $p\text{-value}=0.41$), the distance of 1000 to 1500 km yields
249 an r of 0.18 ($n=24$, $p\text{-value}=0.40$), while a 1500 to 2000 km distance results in an r of 0.1 ($n=21$,
250 $p\text{-value}=0.69$).

251

252 **3.2 Precipitation isotope evolution during TC events**

253

254 Overall, precipitation isotopes associated with TCs mark the lower range of $\delta^{18}\text{O}$ values during
255 the study period. Especially during the 2014 season, precipitation with low isotope values
256 mostly occurred throughout passage of TCs. For instance, Rammasun led to the lowest δ -
257 value (Fig. 5, point a, -13.84 ‰) of the whole study period, while other TCs such as Fung-
258 Wong (Fig. 5, point c, -12.16 ‰), Kalmaegi (Fig. 5, point b, -11.39 ‰), or Hagupit (Fig. 5, point
259 d, -9.88 ‰) caused other negative excursions in isotopic values. The 2015 season is
260 characterized by on average a slightly higher isotopic enrichment during the summer months
261 with heavy rainfall. Nonetheless, a similar noticeable isotope signal is visible with low $\delta^{18}\text{O}$,
262 clustered along the lower end of the sample range, for example, caused by Linfa (Fig. 5, point
263 f, -8.5 ‰) or Koppu (Fig. 5, point i, -8.7 ‰). The other TCs that occurred during the study
264 period and were investigated by us were Mekkhala (Fig. 5, point e, -10.77 ‰), Twelve (Fig. 5,
265 point g, -7.7 ‰) and Mujigae (Fig. 5, point h, -7.5 ‰). However, relatively negative isotope
266 samples (Fig. 5) also originated from non-TC rainfall systems. Those events are discussed
267 below.

268

269 Out of the nine TCs that occurred within a 500 km radius from the sampling site, Rammasun
270 and Kalmaegi left clearly observable, distinct isotopic signatures during their approach and
271 dissipation, which we will therefore present in more detail in the next paragraphs. Typhoon
272 Hagupit (Fig. 5, point d) similarly led to a clear isotopic evolution pattern during its time of
273 occurrence in the Philippines and is shown in the supplementary (S1).

274

275 Typhoon Rammasun's rainfall intensities based on the IMERG precipitation data together
276 with its track from IBTrACKS is shown in Fig. 6a. Typhoon Rammasun stands out in our study
277 period as it moved straight towards the National Capital Region of the Philippines, resulting
278 in a direct hit. Rammasun, locally named Glenda, made landfall in the Bicol region of southern
279 Luzon on 15 July, with wind speeds of about 160 km/h. On 16 July, it passed south of
280 Metropolitan Manila 50 km from our sampling site, with maximum winds of 130 km/h,
281 gradually losing strength over land. As Rammasun approached on 15 July, the precipitation
282 exhibited relatively high $\delta^{18}\text{O}$ of -4 ‰ while rainfall was weak (Fig. 7a). On 16 July, $\delta^{18}\text{O}$ shifted
283 to -13.84 ‰, while the typhoon's track was the closest to our sampling site and rainfall
284 amount was high. As Rammasun moved away, precipitation isotopes became more positive,
285 and rainfall amount decreased. The characteristic isotopic evolution with time related to

286 Rammasun's distance and rainfall intensities can be seen in Fig. 8a, where the different radii
287 indicate the distance to the sampling site, and the strong isotopic depletion observed on 16
288 July is also evident. As Rammasun with its storm centre tracked towards the northwest and
289 away from Metropolitan Manila, our precipitation samples were relatively isotopically
290 enriched for the following two days, namely -9,12 ‰ on 17 July and -6,26 ‰ on 18 July.

291

292 Typhoon Kalmaegi, locally named Luis, was the first typhoon to make landfall in the
293 Philippines two months after Rammasun. Kalmaegi reached typhoon intensity on 13
294 September, making landfall the following day in northern Luzon, with maximum wind speeds
295 of about 120 km/h. Kalmaegi tracked relatively far away from the sampling site (about 350
296 km), but the accumulated rainfall it produced was centred south of the track, placing it
297 considerably closer to the National Capital Region (Fig. 6b). Despite the distance of the eye
298 from the sampling site, a characteristic isotopic pattern was visible, with the most negative
299 $\delta^{18}\text{O}$ value of -11.39 ‰ on 15 September, coincident with the highest rainfall (Fig. 7b). The
300 following day, $\delta^{18}\text{O}$ values returned to higher values with the increase in distance from the
301 eye. This is also seen in a spatial representation in Fig. 8b, visualizing the track of Kalmaegi
302 and the respective $\delta^{18}\text{O}$ values. Kalmaegi was first approaching the sampling site on 14
303 September and passed away on 15 and 16 September. The lowest $\delta^{18}\text{O}$ was observed on 15
304 September and is indicated in the figure in dark blue.

305

306

307 **4. Discussion**

308 **4.1 Stable isotopes of precipitation – a possible tracer for TCs**

309

310 As stable water isotopes fractionate during the physical process of evaporation and
311 condensation, they serve as effective tracers in the hydrological cycle (Dansgaard, 1964; He
312 et al., 2018; Risi et al., 2008; Tremoy et al., 2014). Here, we have demonstrated that stable
313 water isotopes can possibly be used to identify TC activity in the Southeast Asian region by
314 excursions in $\delta^{18}\text{O}$, providing evidence and supporting the hypothesis that TCs may leave a
315 clear isotopic signal in the Philippines. The strong isotopic depletion is due to high
316 condensation efficiencies in cyclonic convective rain bands, leading to extensive
317 fractionation. This is particularly pronounced in intense, large-scale TCs (Lawrence, 1998;

318 Lawrence and Gedzelman, 1996). In the previous section, we have presented our findings of
319 precipitation isotope ratios associated with typhoon activities affecting Metropolitan Manila
320 during the study period of March 2014 to October 2015. Based on our time series, we
321 therefore argue that for the Philippines, the lowest measured isotope value likely indicates
322 the occurrence of a TC, such as is the case for Typhoon Rammasun (Fig. 5). Similarly, other
323 anomalously low $\delta^{18}\text{O}$ values at our site are caused by TC making landfall or passing by.

324

325 Individual TCs (Rammasun and Kalmaegi) were characterized by consistent isotopic
326 excursions to very negative $\delta^{18}\text{O}$ in a range of up to -9 ‰ compared to the mean isotopic
327 value of -5.29 ‰ (Fig. 7 and 8). A TC approaching the sampling site had relatively higher
328 isotope values than at its later stages when it was closest to the site in Metropolitan Manila.
329 When at its closest, strong rainfall together with increased fractionation depleted
330 precipitation isotopes, leading to a distinct drop in isotope value. Such a strong negative
331 isotopic shift in precipitation has been previously observed in other regions (Fudeyasu et al.,
332 2008; Lawrence and Gedzelman, 1996; Munksgaard et al., 2015; Xu et al., 2019). As the TC
333 moved away and rainfall intensities weakened, $\delta^{18}\text{O}$ in precipitation became again more
334 positive, likely due to evaporative effects (Munksgaard et al., 2015; Xu et al., 2019).

335

336 As the strongest TC in terms of wind speeds, damage costs, and fatalities, Typhoon Rammasun
337 reduced $\delta^{18}\text{O}$ most during our study period, to -13.84 ‰. Similarly, Typhoon Kalmaegi led to
338 extensive damage and caused a significantly negative excursion in precipitation $\delta^{18}\text{O}$ to -11.39
339 ‰, suggesting that the lowest isotope values might indicate the occurrence of the strongest
340 TC at that time at our site in the Philippines. We note that our isotopic measurements are
341 similar to observations elsewhere. For example, the range of $\delta^{18}\text{O}$ values caused by Typhoon
342 Shanshan affecting the subtropical Ishigaki Island was -6 to -13 ‰, (Fudeyasu et al., 2008);
343 Tropical Cyclone Ita led to a range of -4.8 to -20.2 ‰ in northeastern Australia (Munksgaard
344 et al., 2015); several TCs which made landfall in Texas resulted in isotope values from -3.9 to
345 -14.3 ‰ (Lawrence and Gedzelman, 1996); or hurricanes that affected Puerto Rico and
346 southern Texas were found to deplete $\delta^{18}\text{O}$ up to -18 ‰ (Lawrence, 1998). The lowest value
347 resulting from Typhoon Phailin on the Andaman Islands was reported to be -5.5 ‰, and
348 Typhoon Lehar depleted the precipitation sample to -17.1 ‰ (Chakraborty et al., 2016). For
349 TCs within a distance of up to 500 km from the sampling site at the University of the

350 Philippines Diliman in Metropolitan Manila we measured an isotopic range of -7.7 ‰
351 (Typhoon Koppu) to -13.84 ‰ (Typhoon Rammasun). Despite the overall comparability to our
352 measurements, differences exist. The lowest values observed in some studies are
353 considerably more negative than at our site (Lawrence, 1998; Munksgaard et al., 2015).
354 However, we attribute these differences to a variety of features, such as the specific climatic
355 condition at each site, differences in temperature, humidity, and altitude or latitude, which
356 are likely contributing factors to the observed isotopic variation by altering isotopic
357 fractionation. Further, rainout history, location of typhoon tracks, topography, respective
358 strength of each TC, as well as its distance to the sampling site most likely have a significant
359 influence as well (Fudeyasu et al., 2008; Good et al., 2014; Munksgaard et al., 2015; Xu et al.,
360 2019).

361

362 We used IMERG satellite precipitation data to assess why other very low isotopic excursions
363 occurred on various days (Fig. 5). IMERG data with its fine spatio-temporal resolution allows
364 the identification of convective rainfall areas and the passage of TCs and other rain systems
365 (Fig. 6). Our analysis shows that precipitation events with anomalously low isotope signals
366 unassociated with TCs are largely related to local, strong convective rainfall events or large
367 scale and slow-moving rain areas passing over the National Capital Region. Therefore, the
368 degree of convection is responsible for the other observed low $\delta^{18}\text{O}$ outliers that are not
369 related to cyclone rainfall, as strong convection and long stratiform rainfall leads to intense
370 fractionation (He et al., 2018; Risi et al., 2008; Tremoy et al., 2014). Contrarily, we speculate
371 that the more positive isotope values clustering along the higher end of the sample spectrum
372 around 0 ‰, are associated with local, short convective rainfall events and light intensity rain
373 as confirmed with IMERG satellite precipitation data. Additionally, the PAGASA rain gauge
374 data indicates that rainfall amounts are very low during days with such very enriched isotope
375 samples, such as 0.3 mm/day for the highest recorded sample of 4 ‰ on 9 April 2014.
376 Interestingly, TCs at our site were found to be related with low isotope values together with
377 high rainfall amounts (Fig. 5), while the majority of other low isotopic values unassociated
378 with TCs were characterized by on average lesser rainfall amounts. This possibly indicates that
379 TCs in the Philippines, besides using for instance modern-day satellite or radar data, can be
380 detected using these two parameters, i.e. strong isotopic depletion coupled with high rainfall
381 amounts.

382

383 The aforementioned local convective precipitation events have the potential to induce a
384 signal of very negative $\delta^{18}\text{O}$, which is not related to TC activities. We therefore label such a
385 signal as a “false non-TC signal”, as it is induced by non-TC rainfall. This results in the fact that
386 TCs occurring during our study period do not entirely cluster along the lowest range of isotope
387 values as seen in Fig. 5. Nevertheless, Typhoon Rammasun caused a clear drop in $\delta^{18}\text{O}$ and
388 stands out in the dataset. This might be the case because Rammasun’s track and heavy rainfall
389 comes in closest proximity (50 km) to the sampling site. Other TCs occurring within the 500
390 km radius did not lead to such a clear negative isotopic signature, likely because these
391 typhoons did not pass the sampling site at all, or heavy rainfall occurred elsewhere within the
392 TC rainfall system (see S 2 for their tracks and accumulated rainfall areas). Some of these TCs
393 have intense rainfall areas over other parts of the Philippines and are characterized by a
394 variable track, likely influenced by land interactions. Land interaction reduces TC strength and
395 can lead to rain out due to orographic effects induced by the north-south oriented mountain
396 ranges (Park et al., 2017; Xie and Zhang, 2012; Xu et al., 2019). Especially Typhoon Koppu
397 rained out before making landfall and abruptly changed its track, instead of passing by
398 Metropolitan Manila. Similarly, Typhoon Mekkhala’s intense rainfall occurred along the
399 eastern coasts before it started to dissipate. Evidently, due to these factors the isotope values
400 associated with those TCs were not as negative as during Rammasun. Therefore, a TC, which
401 is relatively far away from the sampling site, produces an isotope signal that is not as clear
402 and as negative, thus averaging out between the other low values from rain systems
403 unassociated with TC.

404

405 **4.2 Drivers of isotopic variation at Metropolitan Manila**

406

407 $\delta^{18}\text{O}$, $\delta^2\text{H}$, and the second parameter d-excess all show seasonal variabilities and are
408 influenced by several climatic factors, including precipitation amount, temperature, and
409 relative humidity. The scale of their influence varies depending on daily or monthly values.
410 The results indicate that $\delta^{18}\text{O}$ on daily levels is not influenced by temperature, relative
411 humidity, or precipitation amount (Fig. 2) as drivers of isotopic variability. Instead, we
412 speculate that other processes, such as large scale convection and processes at the moisture
413 source region might influence stable isotopes of precipitation at our study site (Conroy et al.,

414 2016; He et al., 2018; Kurita, 2013). Interestingly, $\delta^{18}\text{O}$ is not affected by precipitation amount
415 on short timescales (Fig. 4), which has also been previously confirmed in other tropical
416 regions, suggesting that the tropical amount effect is not reflected on daily timescales
417 (Belgaman et al., 2016; Dansgaard, 1964; He et al., 2018; Kurita et al., 2009; Marryanna et al.,
418 2017; Permana et al., 2016). However, comparing monthly $\delta^{18}\text{O}$ to $\delta^2\text{H}$ and d-excess and to
419 monthly average precipitation, relative humidity and temperature, the results are clearly
420 different (Table 2). These monthly observations show close relationships with each other,
421 especially $\delta^{18}\text{O}$ and precipitation amount are linked (see section 3.1). The close relationship
422 between these two parameters can be attributed to the tropical amount effect (Aggarwal et
423 al., 2012; Bowen, 2008; Conroy et al., 2016). The relatively close relationship with $r=-0.67$
424 between monthly $\delta^{18}\text{O}$ and monthly total precipitation might be likely due to the influence of
425 regional convective activities on the isotopic composition of precipitation (Bony et al., 2008;
426 He et al., 2018; Moerman et al., 2013; Risi et al., 2008).

427

428 **4.3 Distance of TCs from Metropolitan Manila**

429

430 Our observations provide details on spatial distance from the collection site towards TCs'
431 centres, as our findings indicate that the distance from the storm centre to the sampling site
432 impacts the isotopic value (see section 3.1). This suggests that a TC more than 500 km away
433 from the sampling site has no influence on precipitation isotopes (Munksgaard et al., 2015).
434 Thus, the closer the TC is to the sampling site, the more negative the isotope signal and the
435 larger the δ -change. This relationship might provide information on storm structure and
436 intensity, as the intensity increases with proximity of the TC to the sampling location. We thus
437 confirm that the isotope value at our location is a function of the closest approach of the
438 storm's centre to the sampling site (Lawrence and Gedzelman, 1996).

439

440 Figure 9 displays all the precipitation samples associated with TC presence and activities
441 within a 2000 km radius from Metropolitan Manila, and further highlights the relationship
442 between distance and isotopic depletion, additionally providing a spatial indication of TC's
443 quadrants and their tracks relative to the location of the sampling site. Strongest depletion
444 occurs within the 500 km radius. However, two relatively negative outliers are located within
445 a 1000 to 1500 km radius in the northwest quadrant (see points a and b in Fig. 9). These two

446 samples were taken during the passage of tropical storm Kujira on 22nd and 23rd of June 2015
447 (Fig. 5), which was more than 1000 km away from Metropolitan Manila travelling east along
448 the coast of Vietnam as seen with IBTrACKS data. We investigated these two samples with
449 IMERG satellite precipitation data and identified them as a part of a mesoscale system, with
450 strong convective cells delivering intense rainfall, leading to distinct isotopic depletion, and
451 inducing a “false non-TC signal” of very negative $\delta^{18}\text{O}$, which is not related to TC activity.

452

453 **4.4 Cyclone track’s rainfall intensity**

454

455 IMERG satellite precipitation data also reveal that the highest rainfall intensities occur at the
456 left side of the TC track for all the TC within the 500 km radius, except for Hagupit and
457 Mekkhala, which are more complex cases (Fig. 6a, b, supplementary S 2). This is in contrast
458 to the results from Villarini et al. (2011), who found that the largest rainfall accumulation
459 appeared on the right side of the hurricane tracks. They also noted that large rainfall amounts
460 occurred far away from the storm’s track, which we can confirm and quantify with our
461 observations. The largest rainfall totals vary in a range of 50 to 150 km away from the storm’s
462 centre depending on the TC. For Kalmaegi the intense rainfall areas are up to 150 km away
463 from the storm’s centre. These areas with the highest rainfall totals should most likely
464 coincide with the most negative isotope value, indicating that the strongest depletion occurs
465 in the outer cyclonic rain bands. This is consistent with previous findings (Gedzelman et al.,
466 2003; Lawrence and Gedzelman, 1996; Munksgaard et al., 2015). However, Fudeyasu et al.
467 (2008) observed the highest isotope values in the inner eye wall, i.e. in close proximity to the
468 storm’s centre. We could not investigate this further as no TC passed by our site in a distance
469 of about 20 km, which is the size of a typical typhoon’s eye (Weatherford and Gray, 1988).

470

471 **4.5 Implications for paleoclimate studies**

472

473 Isotope proxies from paleoarchives such as tree rings and speleothems have been utilized to
474 reconstruct past cyclone activities (Frappier, 2013; Frappier et al., 2007; Miller et al., 2006;
475 Nott et al., 2007). For instance, stalagmites yielded a record of weekly temporal resolution
476 with negative isotopic excursions related to TC activity (Frappier et al., 2007). Such a high
477 temporal resolution from stalagmites makes our in-situ measurements very comparable,

478 highlighting the potential to use both in conjunction. Similarly, high-resolution tree ring
479 isotope analysis identified the occurrence of Hurricane Ivan and Hurricane Frances in 2004,
480 which both resulted in the lowest observed precipitation isotope values for that year (Li et
481 al., 2011). Nevertheless, it is important to consider possible limitations at the study site that
482 arise in paleotempestology, such as sea level change or disruption of sedimentological
483 records through floods or tsunamis. These need to be evaluated when comparing
484 precipitation isotopes related to TCs with other proxy records such as speleothems and
485 coastal deposits and when choosing the study area (Oliva et al., 2017). However, the
486 aforementioned paleotempestology studies suffer from uncertainty regarding parameters
487 such as TC intensity and distance to the storm's centre affecting the isotope signal. Our study
488 provides further information on these parameters as we hypothesize that immediate
489 proximity of a TC results in very low $\delta^{18}\text{O}$. Therefore, we might aid with a better interpretation
490 of paleoarchives. Moreover, these studies are limited in number and only focus on a few
491 regions affected by TCs, such as Central America and the Southeastern USA (Frappier et al.,
492 2007; Miller et al., 2006). However, more paleotempestology studies investigating
493 paleoarchives related to typhoon footprints covering different regions and countries would
494 provide a better understanding of past TC activity, ultimately resulting in better and more
495 accurate climate reconstructions. TC projections related to climate change could also be
496 improved, which is especially relevant for decision makers dealing with TC related impacts
497 and damages. Our in-situ isotope measurements provide baseline data input in an
498 understudied tropical region, providing isotopic data of TC occurrence and quantifying the
499 isotopic depletion associated with TC activity. Further, our 19-month dataset suggests that
500 the lowest measured isotope value at the Philippines study site is associated with TC activity,
501 resulting in the distinct negative isotopic shift in the time series (Fig. 5). As rain out history,
502 topography, distance of track or rainfall unassociated with TCs can induce a weak or "false
503 non-TC signal", it is important to choose stalagmites or trees as archives based on their
504 location, ideally covering a spatial gradient thus capturing a TC in its full size.

505

506

507 **5. Conclusions**

508

509 Our study demonstrated that a strong, high-energy TC with a track directly approaching and
510 hitting the sampling site leads to a clear isotopic signal in a time series in the Philippines. If
511 the TC is further away, such as more than 500 km from the site, or heavy TC rainfall occurred
512 elsewhere prior of making landfall, the signal is not as clear and might average out between
513 other rainfall events. Other strong convective rainfall events unassociated with TCs may result
514 in similarly low isotope values, and we label these as a weak or “false non-TC signal”.
515 Therefore, the distance of a TC to the sampling site is a key factor in influencing the isotope
516 signal and such a spatial component needs to be considered when interpreting the isotope
517 signal. However, a longer time series isotope record would help to better constrain controlling
518 factors, such as the influence of topography on high-energy TCs. To what extent mountain
519 ranges and low elevation coastal areas shape the TC induced isotope signal needs further
520 investigation. Based on our findings we conclude that the location of precipitation sample
521 collection needs to be chosen strategically. Ideally, several rainwater collection stations
522 should be operated, covering a wide geographical range such as stretching from northern
523 Luzon to its south. With such a spatial gradient coverage, a TC would likely be captured in its
524 full size. Consequently, we aim to expand our time series spatially and temporally.

525

526 Our dataset is the first of such record in the Philippines and provides much needed data in
527 scarcely sampled Southeast Asia. It can be used as a baseline in paleotempestology studies
528 reconstructing past TC history, in conjunction with tree ring and speleothem datasets, as our
529 data suggest that for Metropolitan Manila the lowest measured isotope value is caused by
530 typhoon activity. A higher precipitation sampling frequency on sub-daily levels at several
531 locations would yield more detailed constraints on TC parameters such as storm structure,
532 which we aim to realize in the future.

533

534

535 **Data availability**

536

537 The underlying research data can be accessed via the supplementary document.

538

539

540 **Author Contributions**

541

542 Dominik Jackisch analysed the data and wrote the manuscript. Bi Xuan Yeo contributed to
543 data analysis and improved the manuscript. Adam D. Switzer conceived the idea, reviewed
544 and improved the manuscript. Shaoneng He provided advice, reviewed and improved the
545 manuscript. Danica Cantarero and Fernando P. Siringan collected the precipitation samples
546 and improved the manuscript. Nathalie F. Goodkin reviewed and improved the manuscript.

547

548

549 **Competing interests**

550

551 The authors declare that they have no conflict of interest.

552

553

554 **Acknowledgments**

555

556 This research was supported by the Earth Observatory of Singapore via its funding from the
557 National Research Foundation Singapore and the Singapore Ministry of Education under the
558 Research Centres of Excellence initiative. This work comprises EOS contribution number 422.
559 This study is also the part of IAEA Coordinated Research Project (CRP Code: F31004) on
560 “Stable isotopes in precipitation and paleoclimatic archives in tropical areas to improve
561 regional hydrological and climatic impact model” with IAEA Research Agreement No. 17980.

562

563

564

565

566

567

568

569

570

571

572

573 **References**

574

575 Aggarwal, P. K., Alduchov, O. A., Froehlich, K. O., Araguas-Araguas, L. J., Sturchio, N. C. and
576 Kurita, N.: Stable isotopes in global precipitation: A unified interpretation based on
577 atmospheric moisture residence time, *Geophys. Res. Lett.*, 39(11), 1–6,
578 doi:10.1029/2012GL051937, 2012.

579 Alojado, D. and Padua, D. M.: Costliest Typhoons of the Philippines (1947 - 2014), [online]
580 Available from:
581 [https://www.typhoon2000.ph/stormstats/WPF_CostliestTyphoonsPhilippines_201](https://www.typhoon2000.ph/stormstats/WPF_CostliestTyphoonsPhilippines_2015Ed.pdf)
582 [5Ed.pdf](https://www.typhoon2000.ph/stormstats/WPF_CostliestTyphoonsPhilippines_2015Ed.pdf) (Accessed 17 September 2019), 2015.

583 Belgaman, H., Ichiyanagi, K., Tanoue, M. and Suwarman, R.: Observational Research on
584 Stable Isotopes in Precipitation over Indonesian Maritime Continent, *J. Japanese*
585 *Assoc. Hydrol. Sci.*, 46(1), 7–28, doi:10.4145/jahs.46.7, 2016.

586 Bony, S., Risi, C. and Vimeux, F.: Influence of convective processes on the isotopic
587 composition ($\delta^{18}\text{O}$ and δD) of precipitation and water vapor in the tropics: 1.
588 Radiative-convective equilibrium and Tropical Ocean-Global Atmosphere-Coupled
589 Ocean-Atmosphere Response Experiment (, *J. Geophys. Res. Atmos.*, 113(19), 1–
590 21, doi:10.1029/2008JD009942, 2008.

591 Bowen, G. J.: Spatial analysis of the intra-annual variation of precipitation isotope ratios
592 and its climatological corollaries, *J. Geophys. Res. Atmos.*, 113(5), 1–10,
593 doi:10.1029/2007JD009295, 2008.

594 Chakraborty, S., Sinha, N., Chattopadhyay, R., Sengupta, S., Mohan, P. M. and Datye, A.:
595 Atmospheric controls on the precipitation isotopes over the Andaman Islands, Bay
596 of Bengal, *Sci. Rep.*, 6, 1–11, doi:10.1038/srep19555, 2016.

597 Cinco, T. A., de Guzman, R. G., Hilario, F. D. and Wilson, D. M.: Long-term trends and
598 extremes in observed daily precipitation and near surface air temperature in the
599 Philippines for the period 1951-2010, *Atmos. Res.*, 145–146, 12–26,
600 doi:10.1016/j.atmosres.2014.03.025, 2014.

601 Cinco, T. A., de Guzman, R. G., Ortiz, A. M. D., Delfino, R. J. P., Lasco, R. D., Hilario, F. D.,
602 Juanillo, E. L., Barba, R. and Ares, E. D.: Observed trends and impacts of tropical
603 cyclones in the Philippines, *Int. J. Climatol.*, 36(14), 4638–4650,
604 doi:10.1002/joc.4659, 2016.

605 Conroy, J. L., Noone, D., Cobb, K. M., Moerman, J. W. and Konecky, B. L.: Paired stable
606 isotopologues in precipitation and vapor: A case study of the amount effect within
607 western tropical Pacific storms, *J. Geophys. Res.*, 121(7), 3290–3303,
608 doi:10.1002/2015JD023844, 2016.

609 Craig, H.: Isotopic variations in meteoric waters, *Science (80-.)*, 133(3465), 1702–1703,
610 doi:10.1126/science.133.3465.1702, 1961.

611 Cruz, F. T., Narisma, G. T., Villafuerte, M. Q., Cheng Chua, K. U. and Olaguera, L. M.: A
612 climatological analysis of the southwest monsoon rainfall in the Philippines,
613 *Atmos. Res.*, 122, 609–616, doi:10.1016/j.atmosres.2012.06.010, 2013.

614 Dansgaard, W.: Stable isotopes in precipitation, *Tellus*, 16(4), 436–468,
615 doi:10.3402/tellusa.v16i4.8993, 1964.

616 Emanuel, K.: Increasing destructiveness of tropical cyclones over the past 30 years,
617 *Nature*, 436(7051), 686–688, doi:10.1038/nature03906, 2005.

618 Frappier, A. B.: Masking of interannual climate proxy signals by residual tropical cyclone
619 rainwater: Evidence and challenges for low-latitude speleothem paleoclimatology,
620 *Geochemistry, Geophys. Geosystems*, 14(9), 3632–3647, doi:10.1002/ggge.20218,
621 2013.

622 Frappier, A. B., Sahagian, D., Carpenter, S. J., González, L. A. and Frappier, B. R.: Stalagmite
623 stable isotope record of recent tropic cyclone events, *Geology*, 35(2), 111–114,
624 doi:10.1130/G23145A.1, 2007.

625 Fudeyasu, H., Ichiyanagi, K., Sugimoto, A., Yoshimura, K., Ueta, A., Yamanaka, M. D. and
626 Ozawa, K.: Isotope ratios of precipitation and water vapor observed in typhoon
627 Shanshan, *J. Geophys. Res. Atmos.*, 113(12), 1–9, doi:10.1029/2007JD009313,
628 2008.

629 Gedzelman, S., Lawrence, J., Gamache, J., Black, M., Hindman, E., Black, R., Dunion, J.,
630 Willoughby, H. and Zhang, X.: Probing Hurricanes with Stable Isotopes of Rain and
631 Water Vapor, *Mon. Weather Rev.*, 131(6), 1112–1127, doi:10.1175/1520-
632 0493(2003)131<1112:PHWSIO>2.0.CO;2, 2003.

633 Van Geldern, R. and Barth, J. A. C.: Optimization of instrument setup and post-run
634 corrections for oxygen and hydrogen stable isotope measurements of water by
635 isotope ratio infrared spectroscopy (IRIS), *Limnol. Oceanogr. Methods*, 10, 1024–
636 1036, doi:10.4319/lom.2012.10.1024, 2012.

637 Good, S. P., Mallia, D. V., Lin, J. C. and Bowen, G. J.: Stable isotope analysis of precipitation
638 samples obtained via crowdsourcing reveals the spatiotemporal evolution of
639 superstorm sandy, *PLoS One*, 9(3), doi:10.1371/journal.pone.0091117, 2014.

640 Gröning, M., Lutz, H. O., Roller-Lutz, Z., Kralik, M., Gourcy, L. and Pölsenstein, L.: A simple
641 rain collector preventing water re-evaporation dedicated for $\delta^{18}\text{O}$ and $\delta^2\text{H}$
642 analysis of cumulative precipitation samples, *J. Hydrol.*, 448–449, 195–200,
643 doi:10.1016/j.jhydrol.2012.04.041, 2012.

644 Guan, S., Li, S., Hou, Y., Hu, P., Liu, Z. and Feng, J.: Increasing threat of landfalling
645 typhoons in the western North Pacific between 1974 and 2013, *Int. J. Appl. Earth*
646 *Obs. Geoinf.*, 68(7), 279–286, doi:10.1016/j.jag.2017.12.017, 2018.

647 He, S., Goodkin, N. F., Jackisch, D., Ong, M. R. and Samanta, D.: Continuous real-time
648 analysis of the isotopic composition of precipitation during tropical rain events:
649 Insights into tropical convection, *Hydrol. Process.*, 32(11), 1531–1545,
650 doi:10.1002/hyp.11520, 2018.

651 Huffman, G. J., Bolvin, D., Braithwaite, D., Hsu, K., Joyce, R., Kidd, C., Nelkin, E. J.,
652 Sorooshian, S., Tan, J. and Xie, P.: Algorithm Theoretical Basis Document (ATBD) of
653 Integrated Multi-satellite Retrievals for GPM (IMERG), version 4.6, Nasa [online]
654 Available from:
655 https://pmm.nasa.gov/sites/default/files/document_files/IMERG_ATBD_V4.6.pdf
656 (Accessed 11 September 2019), 2017.

657 Knapp, K. R., Levinson, D. H., Kruk, M. C., Howard, J. H. and Kossin, J. P.: The International
658 Best Track Archive for Climate Stewardship (IBTrACS), *Bull. Am. Meteorol. Soc.*, 91,
659 363–376, doi:10.1007/978-90-481-3109-9_26, 2010.

660 Kurita, N.: Water isotopic variability in response to mesoscale convective system over the
661 tropical ocean, *J. Geophys. Res. Atmos.*, 118(18), 10376–10390,
662 doi:10.1002/jgrd.50754, 2013.

663 Kurita, N., Ichiyanagi, K., Matsumoto, J., Yamanaka, M. D. and Ohata, T.: The relationship
664 between the isotopic content of precipitation and the precipitation amount in
665 tropical regions, *J. Geochemical Explor.*, 102(3), 113–122,
666 doi:10.1016/j.gexplo.2009.03.002, 2009.

667 Lagmay, A. M. F., Agaton, R. P., Bahala, M. A. C., Briones, J. B. L. T., Cabacaba, K. M. C.,
668 Caro, C. V. C., Dasallas, L. L., Gonzalo, L. A. L., Ladiero, C. N., Lapidez, J. P., Mungcal,

669 M. T. F., Puno, J. V. R., Ramos, M. M. A. C., Santiago, J., Suarez, J. K. and Tablazon,
670 J. P.: Devastating storm surges of Typhoon Haiyan, *Int. J. Disaster Risk Reduct.*, 11,
671 1–12, doi:10.1016/j.ijdrr.2014.10.006, 2015.

672 Lawrence, J. R.: Isotopic spikes from tropical cyclones in surface waters: Opportunities in
673 hydrology and paleoclimatology, *Chem. Geol.*, 144(1–2), 153–160,
674 doi:10.1016/S0009-2541(97)00090-9, 1998.

675 Lawrence, J. R. and Gedzelman, S. D.: Low stable isotope ratios of tropical cyclone rains,
676 *Geophys. Res. Lett.*, 23(5), 527–530, 1996.

677 Lawrence, J. R., Gedzelman, S. D., Gamache, J. and Black, M.: Stable isotope ratios:
678 Hurricane Olivia, *J. Atmos. Chem.*, 41(1), 67–82, doi:10.1023/A:1013808530364,
679 2002.

680 Li, Z. H., Labbé, N., Driese, S. G. and Grissino-Mayer, H. D.: Micro-scale analysis of tree-
681 ring $\delta^{18}\text{O}$ and $\delta^{13}\text{C}$ on α -cellulose spline reveals high-resolution intra-annual
682 climate variability and tropical cyclone activity, *Chem. Geol.*, 284(1–2), 138–147,
683 doi:10.1016/j.chemgeo.2011.02.015, 2011.

684 Marryanna, L., Kosugi, Y., Itoh, M., Noguchi, S., Takanashi, S., Katsuyama, M., Tani, M. and
685 Siti-Aisah, S.: Temporal variation in the stable isotopes in precipitation related to
686 the rainfall pattern in a tropical rainforest in Peninsular Malaysia, *J. Trop. For. Sci.*,
687 29(3), 349–362, doi:10.26525/jtfs2017.29.3.349362, 2017.

688 Mei, W., Xie, S. P., Primeau, F., McWilliams, J. C. and Pasquero, C.: Northwestern Pacific
689 typhoon intensity controlled by changes in ocean temperatures, *Sci. Adv.*, 1(4), 1–
690 8, doi:10.1126/sciadv.1500014, 2015.

691 Miller, D. L., Mora, C. I., Grissino-Mayer, H. D., Mock, C. J., Uhle, M. E. and Sharp, Z.: Tree-
692 ring isotope records of tropical cyclone activity., *Proc. Natl. Acad. Sci. U. S. A.*,
693 103(39), 14294–14297, doi:10.1073/pnas.0606549103, 2006.

694 Moerman, J. W., Cobb, K. M., Adkins, J. F., Sodemann, H., Clark, B. and Tuen, A. A.: Diurnal
695 to interannual rainfall $\delta^{18}\text{O}$ variations in northern Borneo driven by regional
696 hydrology, *Earth Planet. Sci. Lett.*, 369–370, 108–119,
697 doi:10.1016/j.epsl.2013.03.014, 2013.

698 Munksgaard, N. C., Zwart, C., Kurita, N., Bass, A., Nott, J. and Bird, M. I.: Stable Isotope
699 Anatomy of Tropical Cyclone Ita, North-Eastern Australia, April 2014, *PLoS One*,
700 10(3), 1–15, doi:10.1371/journal.pone.0119728, 2015.

701 NDRRMC: SitRep No. 38 re Effects of Typhoon “Pablo” (Bopha), [online] Available from:
702 [http://www.ndrrmc.gov.ph/attachments/article/2245/SitRep_No_38_Effects_of_T](http://www.ndrrmc.gov.ph/attachments/article/2245/SitRep_No_38_Effects_of_Typhoon_PABLO_as_of_25DEC2012_0600H.pdf)
703 [yphoon_PABLO_as_of_25DEC2012_0600H.pdf](http://www.ndrrmc.gov.ph/attachments/article/2245/SitRep_No_38_Effects_of_Typhoon_PABLO_as_of_25DEC2012_0600H.pdf) (Accessed 18 September 2019),
704 2012.

705 NDRRMC: Final Report re Effects of Typhoon “Glenda” (RAMMASUN), [online] Available
706 from:
707 [http://ndrrmc.gov.ph/attachments/article/1293/Effects_of_Typhoon_Glenda_\(RA](http://ndrrmc.gov.ph/attachments/article/1293/Effects_of_Typhoon_Glenda_(RAMMASUN)_Final_Report_16SEP2014.pdf)
708 [MMASUN\)_Final_Report_16SEP2014.pdf](http://ndrrmc.gov.ph/attachments/article/1293/Effects_of_Typhoon_Glenda_(RAMMASUN)_Final_Report_16SEP2014.pdf) (Accessed 17 September 2019), 2014.

709 NDRRMC: Final Report re Preparedness Measures and Effects of Typhoon “Lando” (I.N.
710 Koppu), [online] Available from:
711 [http://ndrrmc.gov.ph/attachments/article/2607/FINAL_REPORT_re_Preparedness](http://ndrrmc.gov.ph/attachments/article/2607/FINAL_REPORT_re_Preparedness_Measures_and_Effects_of_Typhoon_LANDO_KOPPU_as_of_14_-_21OCT2015.pdf)
712 [_Measures_and_Effects_of_Typhoon_LANDO_KOPPU_as_of_14_-_21OCT2015.pdf](http://ndrrmc.gov.ph/attachments/article/2607/FINAL_REPORT_re_Preparedness_Measures_and_Effects_of_Typhoon_LANDO_KOPPU_as_of_14_-_21OCT2015.pdf)
713 (Accessed 17 September 2019), 2015.

714 Nott, J., Haig, J., Neil, H. and Gillieson, D.: Greater frequency variability of landfalling
715 tropical cyclones at centennial compared to seasonal and decadal scales, *Earth*
716 *Planet. Sci. Lett.*, 255, 367–372, doi:10.1016/j.epsl.2006.12.023, 2007.

717 Oliva, F., Peros, M. and Viau, A.: A review of the spatial distribution of and analytical
718 techniques used in paleotempestological studies in the western North Atlantic
719 Basin, *Prog. Phys. Geogr.*, 41(2), 171–190, doi:10.1177/0309133316683899, 2017.

720 Pape, J. R., Banner, J. L., Mack, L. E., Musgrove, M. L. and Guilfoyle, A.: Controls on oxygen
721 isotope variability in precipitation and cave drip waters, central Texas, USA, *J.*
722 *Hydrol.*, 385(1–4), 203–215, doi:10.1016/j.jhydrol.2010.02.021, 2010.

723 Park, M. S., Lee, M. I., Kim, D., Bell, M. M., Cha, D. H. and Elsberry, R. L.: Land-based
724 convection effects on formation of tropical cyclone Mekkhala (2008), *Mon.*
725 *Weather Rev.*, 145(4), 1315–1337, doi:10.1175/MWR-D-16-0167.1, 2017.

726 Permana, D. S., Thompson, L. G. and Setyadi, G.: *Journal of Geophysical Research : Oceans*, , 1–18, doi:10.1002/2015JC011534.Received, 2016.

728 Philippine Statistics Authority: Philippine Population Surpassed the 100 Million Mark
729 (Results from the 2015 Census of Population), [online] Available from:
730 <http://www.psa.gov.ph/population-and-housing/node/120080> (Accessed 15
731 September 2019), 2017.

732 Poméon, T., Jackisch, D. and Diekrüger, B.: Evaluating the performance of remotely

733 sensed and reanalysed precipitation data over West Africa using HBV light, J.
734 Hydrol., 547, doi:10.1016/j.jhydrol.2017.01.055, 2017.

735 Rios Gaona, M. F., Villarini, G., Zhang, W. and Vecchi, G. A.: The added value of IMERG in
736 characterizing rainfall in tropical cyclones, *Atmos. Res.*, 209, 95–102,
737 doi:10.1016/j.atmosres.2018.03.008, 2018.

738 Risi, C., Bony, S., Vimeux, F., Descroix, L., Ibrahim, B., Lebreton, E., Mamadou, I. and
739 Sultan, B.: What controls the isotopic composition of the African monsoon
740 precipitation? Insights from event-based precipitation collected during the 2006
741 AMMA field campaign, *Geophys. Res. Lett.*, 35(24), 1–6,
742 doi:10.1029/2008GL035920, 2008.

743 Soria, J. L. A., Switzer, A. D., Villanoy, C. L., Fritz, H. M., Bilgera, P. H. T., Cabrera, O. C.,
744 Siringan, F. P., Maria, Y. Y. S., Ramos, R. D. and Fernandez, I. Q.: Repeat storm
745 surge disasters of typhoon haiyan and its 1897 predecessor in the Philippines, *Bull.*
746 *Am. Meteorol. Soc.*, 97(1), 31–48, doi:10.1175/BAMS-D-14-00245.1, 2016.

747 Takagi, H. and Esteban, M.: Statistics of tropical cyclone landfalls in the Philippines:
748 unusual characteristics of 2013 Typhoon Haiyan, *Nat. Hazards*, 80(1), 211–222,
749 doi:10.1007/s11069-015-1965-6, 2016.

750 Tremoy, G., Vimeux, F., Soumana, S., Souley, I. and Risi, C.: Clustering mesoscale
751 convective systems with laser-based water vapor d18O monitoring in Niamey
752 (Niger), *J. Geophys. Res. Atmos. Res.*, 5079–5103,
753 doi:10.1002/2013JD020968.Received, 2014.

754 Villafuerte, M. Q., Matsumoto, J., Akasaka, I., Takahashi, H. G., Kubota, H. and Cinco, T. A.:
755 Long-term trends and variability of rainfall extremes in the Philippines, *Atmos.*
756 *Res.*, 137, 1–13, doi:10.1016/j.atmosres.2013.09.021, 2014.

757 Villarini, G., Smith, J. A., Baeck, M. L., Marchok, T. and Vecchi, G. A.: Characterization of
758 rainfall distribution and flooding associated with U.S. landfalling tropical cyclones:
759 Analyses of Hurricanes Frances, Ivan, and Jeanne (2004), *J. Geophys. Res. Atmos.*,
760 116(23), 1–19, doi:10.1029/2011JD016175, 2011.

761 Weatherford, C. L. and Gray, W. M.: Typhoon Structure as Revealed by Aircraft
762 Reconnaissance. Part I: Data Analysis and Climatology, *Mon. Weather Rev.*, 116(5),
763 1032–1043, doi:10.1175/1520-0493(1988)116<1032:TSARBA>2.0.CO;2, 1988.

764 Webster, P. J., Holland, G. J., Curry, J. A. and Chang, H.-R.: Changes in Tropical Cyclone

765 Number, Duration, and Intensity in a Warming Environment, *Science* (80-.),,
766 309(4), 1844–1846, doi:10.1126/science.1116448, 2005.

767 Woodruff, J. D., Irish, J. L. and Camargo, S. J.: Coastal flooding by tropical cyclones and
768 sea-level rise, *Nature*, 504(7478), 44–52, doi:10.1038/nature12855, 2013.

769 Xie, B. and Zhang, F.: Impacts of typhoon track and Island topography on the heavy
770 rainfalls in Taiwan associated with Morakot (2009), *Mon. Weather Rev.*, 140(10),
771 3379–3394, doi:10.1175/MWR-D-11-00240.1, 2012.

772 Xu, T., Sun, X., Hong, H., Wang, X., Cui, M., Lei, G., Gao, L., Liu, J., Lone, M. A. and Jiang, X.:
773 Stable isotope ratios of typhoon rains in Fuzhou , Southeast China , during 2013 –
774 2017, *J. Hydrol.*, 570, 445–453, doi:10.1016/j.jhydrol.2019.01.017, 2019.

775
776
777
778
779
780
781
782
783
784
785
786
787
788
789
790
791
792
793
794
795
796

797 **Figures and Captions**

798

799

800

801

802

803

804

805

806

807

808

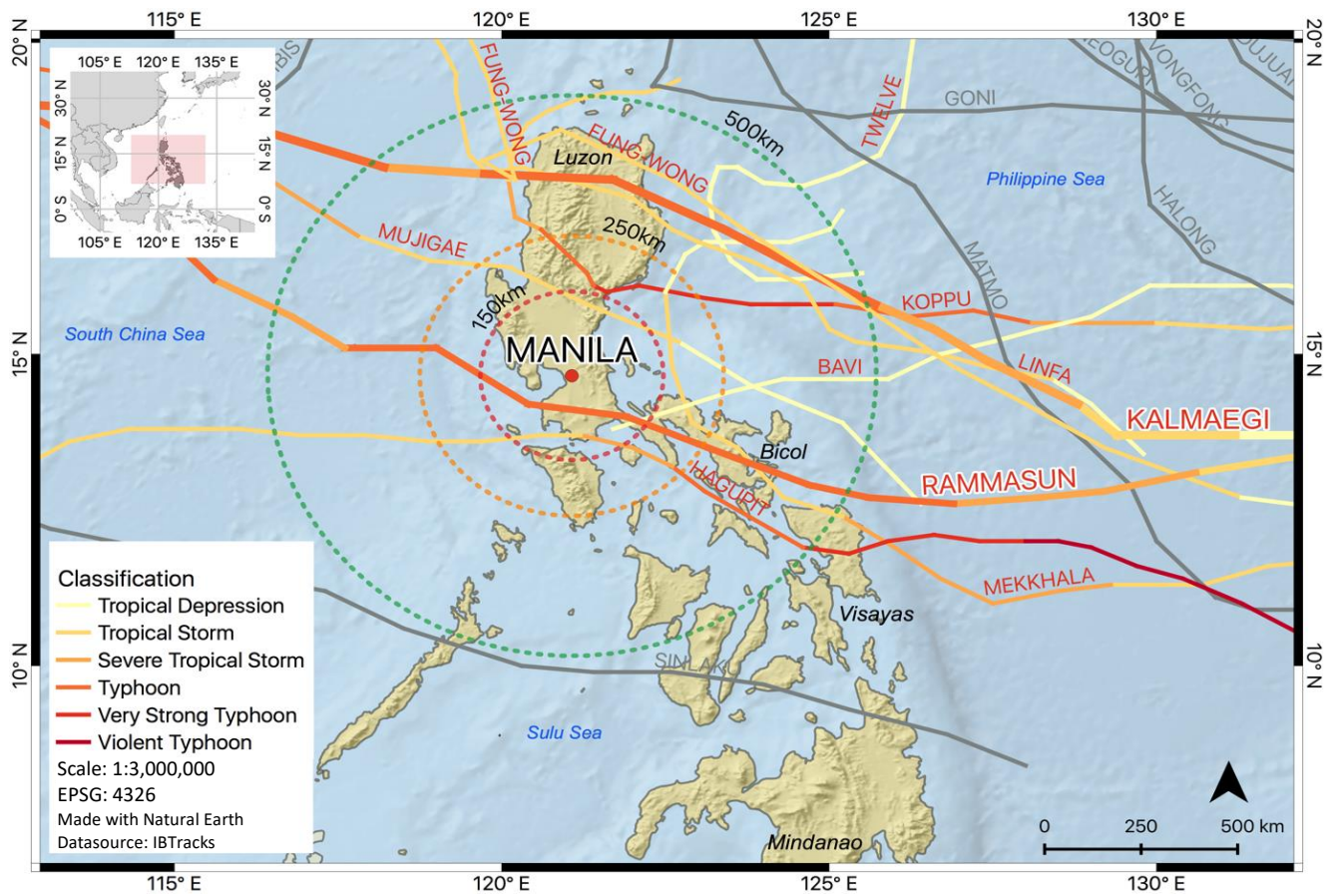
809

810

811

812

813



814

815 **Figure 1 Metropolitan Manila sampling site and TC tracks of 2014 and 2015 seasons.** Three different sized circles indicate the
 816 distance to the sampling site with the outermost one being 500 km in radius. Cyclone tracks are colour-coded according to the
 817 typhoon classification from Regional Specialized Meteorological Center (RSMC) Tokyo. Cyclones in gray colour refer to TC outside
 818 the 500 km radius.

819

820

821

822

823

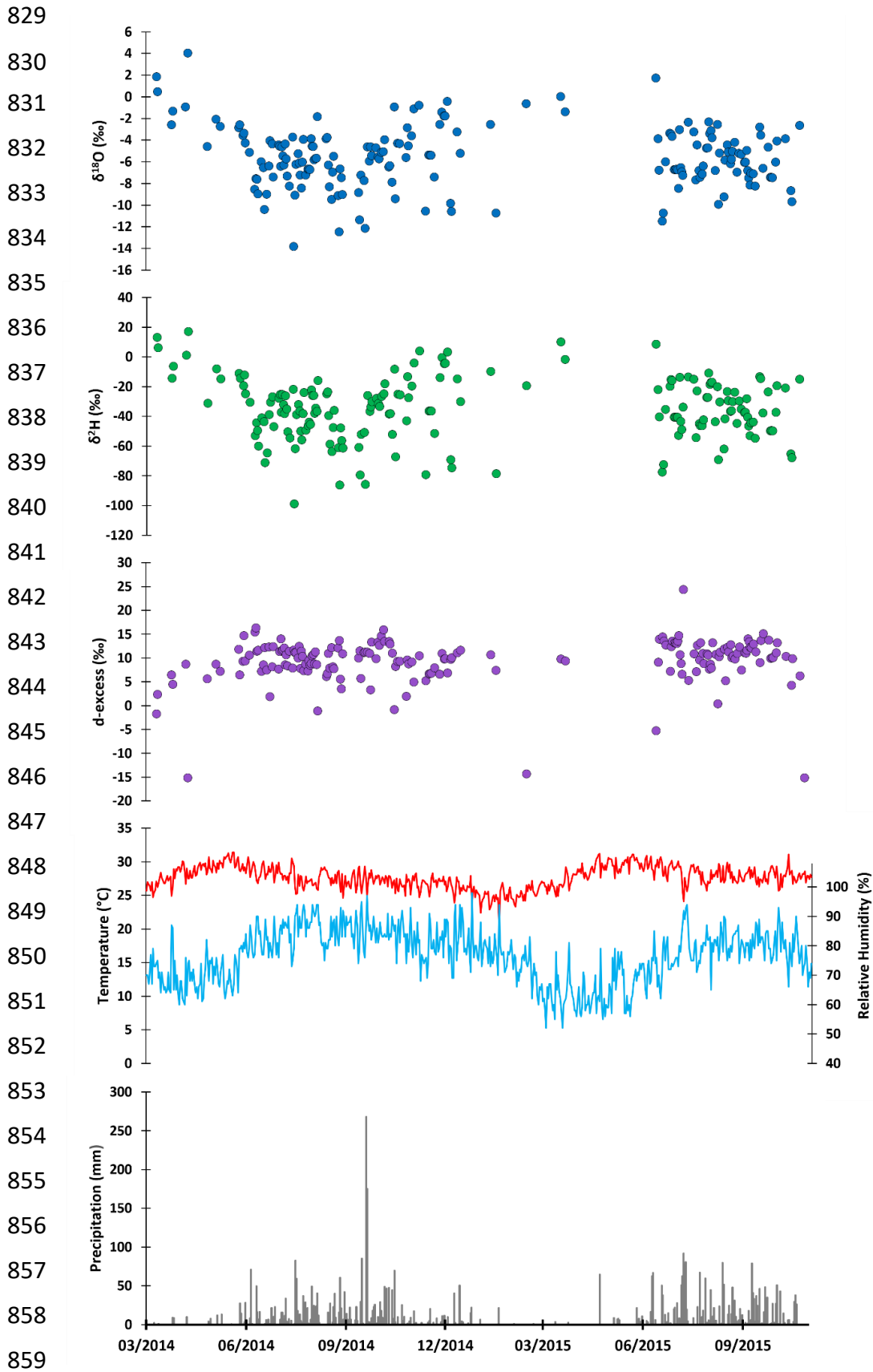
824

825

826

827

828



860 **Figure 2** Time series of daily variations of $\delta^{18}\text{O}$, $\delta^2\text{H}$, d-excess, temperature, relative humidity and precipitation amount
 861 at Metropolitan Manila, Philippines.

862
863
864
865
866
867
868
869
870
871
872
873
874
875
876
877
878
879
880
881
882
883
884
885
886
887
888
889
890
891
892
893

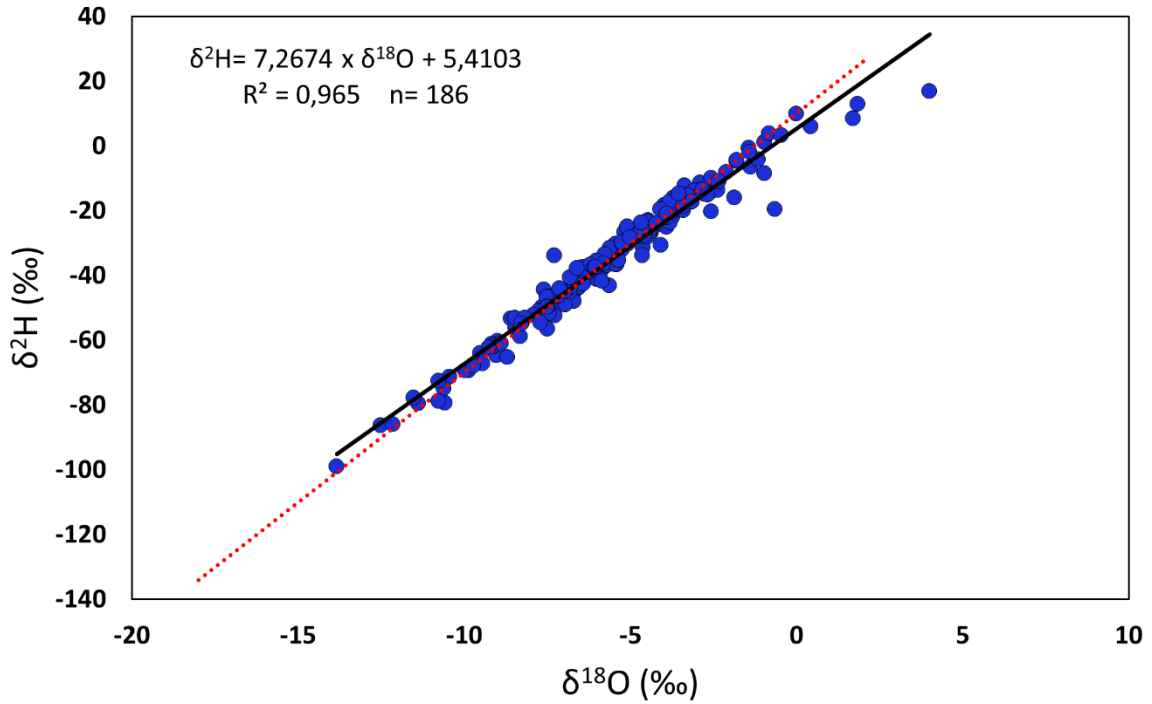


Figure 3 Local meteoric water line (LMWL) established for Metropolitan Manila, Philippines. The red dotted line represents the global meteoric water line (GMWL) ($\delta^2\text{H} = 8 \times \delta^{18}\text{O} + 10$; Craig, 1961).

894
895
896
897
898
899
900
901
902
903
904
905
906
907
908
909
910
911
912
913
914
915
916
917
918
919
920
921
922
923
924
925

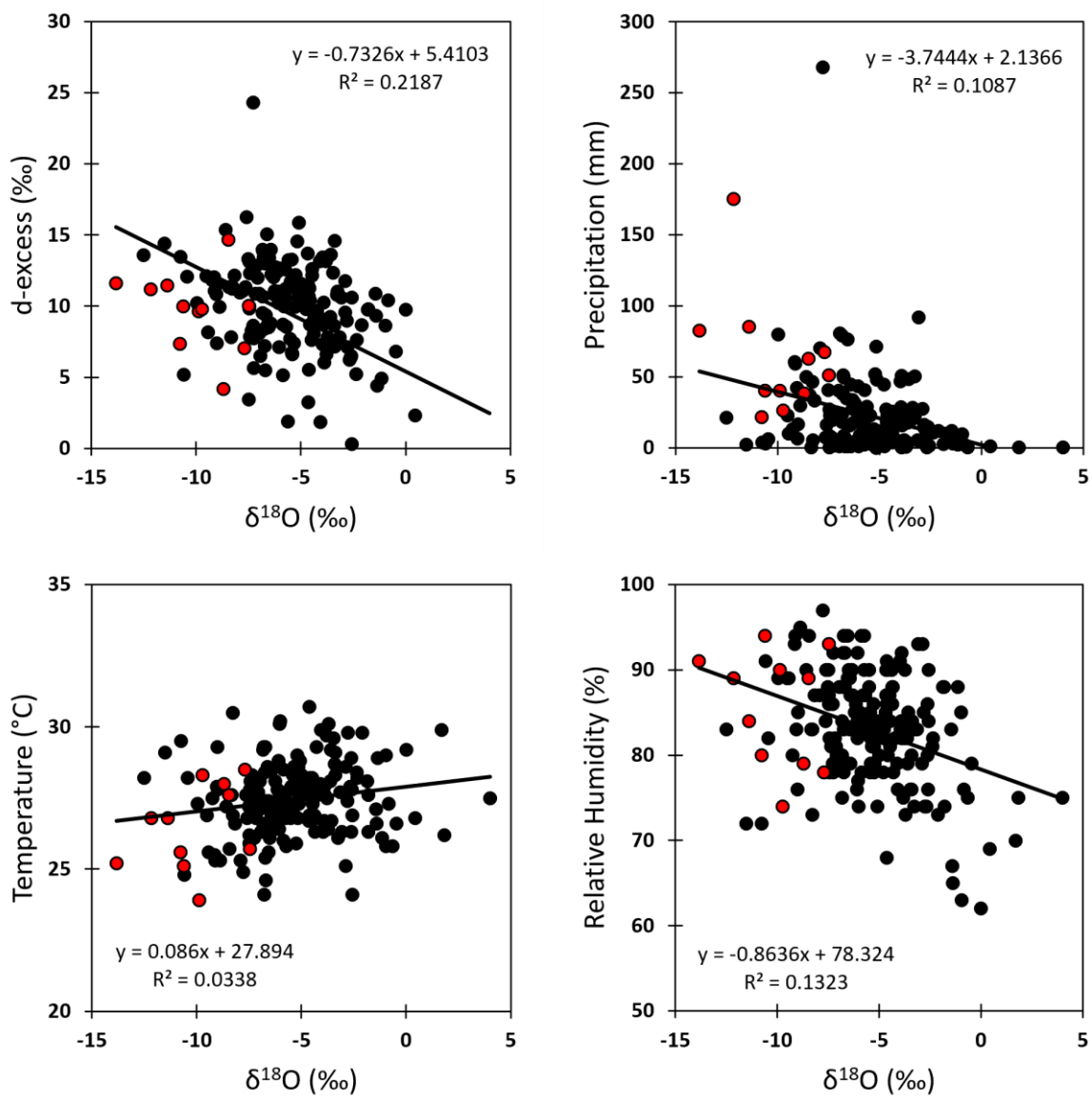


Figure 4 Correlations between daily $\delta^{18}\text{O}$ values and daily values of d-excess, precipitation amount, temperature and relative humidity. Linear regression line, correlation coefficient (R^2), slope and intercept are shown in each plot. Samples associated to TC are shown in red colour similar to Figure 5.

926
 927
 928
 929
 930
 931
 932
 933
 934
 935
 936
 937
 938
 939
 940
 941
 942
 943
 944
 945
 946
 947
 948
 949
 950
 951
 952
 953
 954
 955
 956
 957

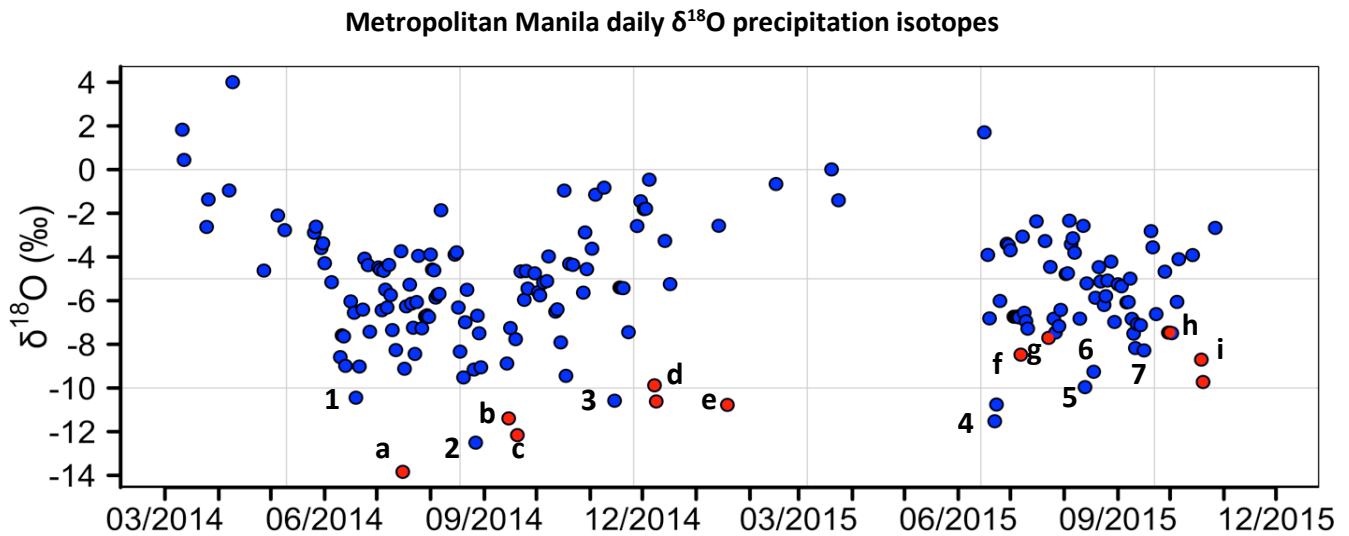


Figure 5 Complete time series of 186 precipitation samples taken between 10 March 2014 to 27 October 2015. $\delta^{18}\text{O}$ data points associated with TC activity are coloured in red. Other anomalously low $\delta^{18}\text{O}$ values were investigated using IMERG satellite precipitation data. a: Rammasun 16/07/14, -13.84 ‰, 83 mm. b: Kalmaegi 15/09/14, -11.39 ‰, 85 mm. c: Fung-Wong 20/09/14, -12.16 ‰, 175 mm. d: Hagupit 8-9/12/14, -9.88 ‰, -10.62 ‰, 40 mm. e: Mekkhala 19/1/15, -10.77 ‰, 22 mm. f: Linfa 07/07/15, -8.5 ‰, 63 mm. g: Twelve 23/07/15, -7.7 ‰, 68 mm. h: Mujigae 01/10/15, -7.5 ‰, 51 mm. i: Koppu 19-20/10/15. -8.7 ‰, -9.72 ‰, 38 mm, 26 mm. 1: storm passing by 19/06/14, -10.44 ‰, 6 mm. 2: large rain areas 27/08/14, -12.5 ‰, 21 mm 3: storm passing by 15/11/14 -10.58 ‰, 3 mm. 4: large rain areas, 22-23/06/15 -10.76 ‰, -11.52 ‰, 2 mm, 4 mm. 5: heavy rainfall 13/08/15, -9.96 ‰, 80 mm. 6: heavy rainfall 18/08/15, -9.26 ‰, 13 mm. 7: local convection 16/09/15, -8.28 ‰, 47 mm.

958
 959
 960
 961
 962
 963
 964
 965
 966
 967
 968
 969
 970
 971
 972
 973
 974
 975
 976
 977
 978
 979
 980
 981
 982
 983
 984
 985
 986
 987
 988
 989

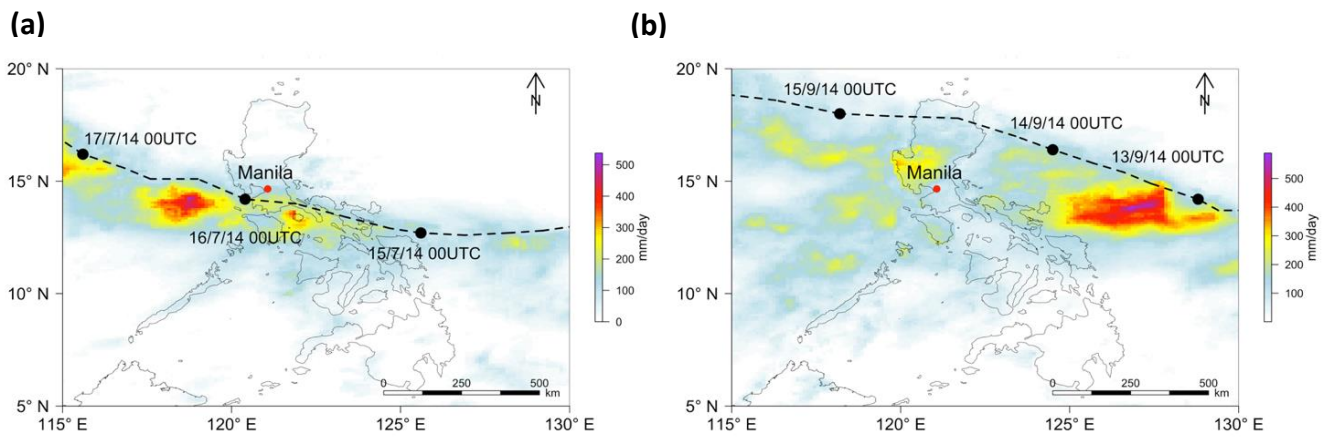


Figure 6 Accumulated precipitation from IMERG satellite data and TC tracks from IBTRACKS for a) Rammasun with precipitation accumulation for 14-17 July 2014, b) Kalmaegi with accumulated precipitation for 12-15 September 2014. Made with base layers from Natural Earth.

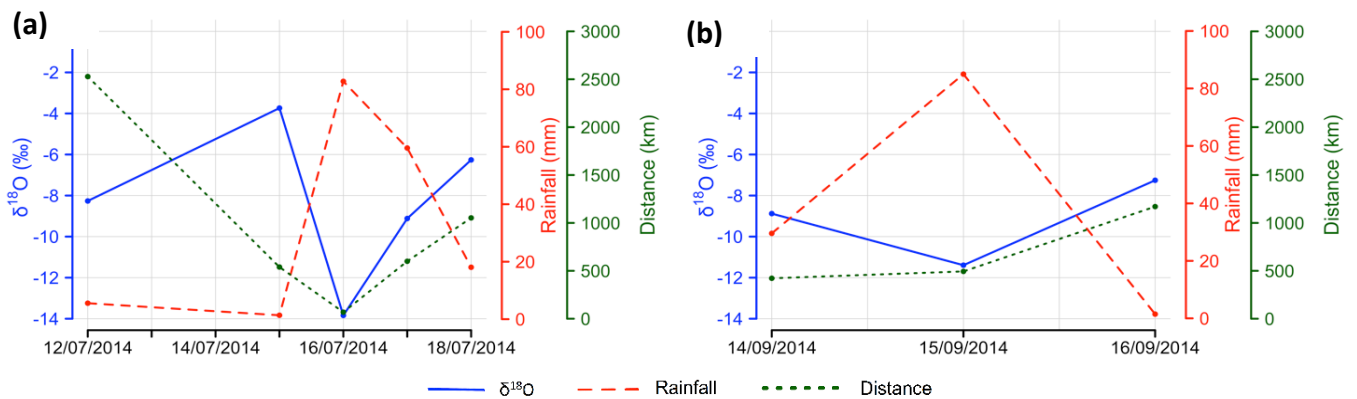
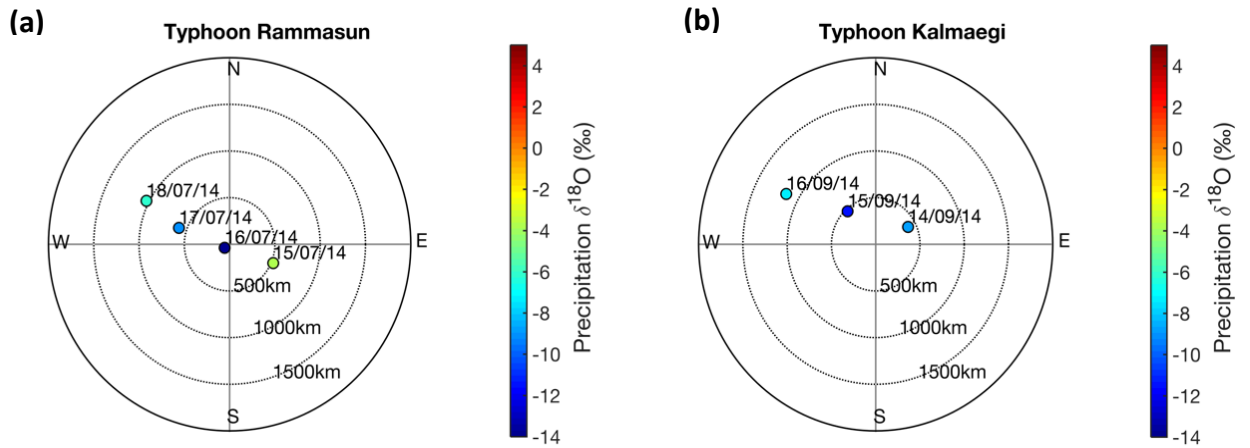


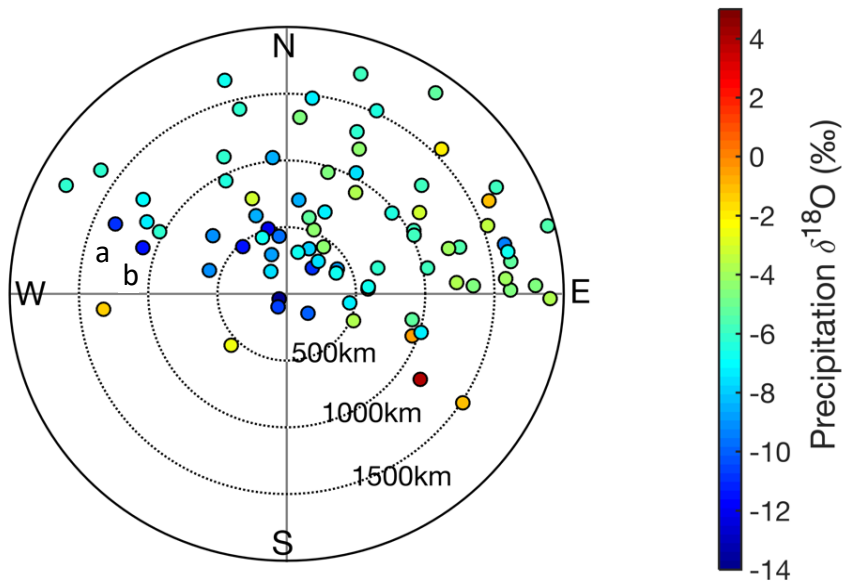
Figure 7 Isotopic signature from TCs during their passage to the Metropolitan Manila sampling site. $\delta^{18}\text{O}$ (blue colour), distance from storm centre to sampling location (green) and daily rainfall amount (red). a) Rammasun, b) Kalmaegi

990
991
992
993
994
995
996
997
998
999



1000 **Figure 8 Spatio-temporal evolution of $\delta^{18}\text{O}$ isotopes.** Centred on Metropolitan Manila collection site, different radii provide
1001 information on distance between storm's centre to Metropolitan Manila. $\delta^{18}\text{O}$ values are colour-coded. a) Rammasun, b) Kalmaegi

1002
1003
1004
1005
1006
1007
1008
1009
1010
1011
1012
1013
1014
1015
1016



1017 **Figure 9 Spatio-temporal variation of isotopes** related to TC activity within 2000 km, with different radii indicating the distance towards
1018 Metropolitan Manila. $\delta^{18}\text{O}$ values are colour-coded.

1019
1020
1021

1022 **Tables**

1023

1024 **Table 1 Costliest typhoons in the Philippines.** Two devastating typhoons, Rammasun and Koppu (ranking 3 and 7),
 1025 occurred during our study period and made landfall. Damage in USD based on each time of TC occurrence (not adjusted to
 1026 current inflation rates).

Rank	Name (local name)	Category (Saffir Simpson scale)	Period of occurrence	Damage in USD	Fatalities	Part of our dataset
1.	Haiyan (Yolanda)	Category 5	2-11 November 2013	~ 2.06 billion USD	~ 6000	No
2.	Bopha (Pablo)	Category 5	2-10 December 2012	~ 977 million USD	1067	No
3.	Rammasun (Glenda)	Category 5	12-17 July 2014	~ 880 million USD	106	Yes
7.	Koppu (Lando)	Category 4	12-21 October 2015	~ 310 million USD	62	Yes

References: Alojado and Padua, 2015; Lagmay et al., 2015; NDRRMC, 2012, 2014, 2015; Soria et al., 2016

1027

1028

1029

1030

1031 **Table 2 Monthly average values of the 19-month time series** of $\delta^{18}\text{O}$, $\delta^2\text{H}$, d-excess and meteorological parameters
 1032 (temperature and relative humidity) except precipitation values are reported as monthly totals.

Month	$\delta^{18}\text{O}$ (‰)	$\delta^2\text{H}$ (‰)	d-excess (‰)	Precipitation (mm)	Temperature (°C)	Relative humidity (%)
Mar 14	-0.43	-0.62	2.82	19.2	27.1	70.0
Apr 14	-0.53	-4.54	-0.33	22.6	28.8	68.9
May 14	-2.89	-13.50	9.63	99.1	29.8	71.7
Jun 14	-6.90	-44.90	10.28	239.1	28.7	81.2
Jul 14	-6.46	-41.68	10.04	455.4	27.5	86.6
Aug 14	-6.39	-42.63	8.51	420.7	27.4	85.7
Sep 14	-7.29	-48.57	9.76	654.9	27.4	85.3
Oct 14	-5.24	-31.73	10.19	406.4	26.9	84.2
Nov 14	-4.39	-27.64	7.48	90.5	26.9	80.0
Dec 14	-4.72	-28.00	9.79	154.6	26.0	81.4
Jan 15	-6.67	-44.41	8.97	29.2	24.6	77.8
Feb 15	-0.66	-19.70	-14.41	2.7	25.5	70.7
Mar 15	-0.70	3.95	9.54	6.6	26.8	62.9
Apr 15				64.8	29.1	62.0
May 15				74.6	29.7	68.4
Jun 15	-5.52	-34.47	9.71	328.7	29.3	73.1
Jul 15	-6.04	-36.69	11.61	28.6	27.8	80.5
Aug 15	-5.25	-32.28	9.74	459.3	28.0	81.1
Sep 15	-6.12	-37.07	11.86	444.8	28.0	81.0
Oct 15	-6.27	-40.80	6.60	250.5	27.8	78.0

1033

1034